THROUGH-THE-WALL TARGET LOCALIZATION WITH TIME REVERSAL MUSIC METHOD

W. Zhang and A. Hoorfar

Antenna Research Laboratory
Center for Advanced Communications
Villanova University
Villanova, PA 19085, USA

L. Li

Department of Petroleum Engineering
Texas A&M University
College Station, TX 77843, USA

Abstract—Time Reversal Multiple Signal Classification (TR-MUSIC) method is studied and adapted for the detection and localization of multiple targets behind the wall in this paper. TR-MUSIC does not involve the FDTD solver for the implementation of the backpropagation of the time reversed field and is very computational efficient. The Green's function vectors for the computation of the TR-MUSIC pseudo-spectrum is efficiently evaluated with the saddle point method for a homogeneous wall. By employing the null space of the multistatic response matrix, simultaneous localization of multiple targets behind the wall can be achieved by TR-MUSIC method. Numerical results are presented to show the effectiveness of through-the-wall imaging (TWI) with TR-MUSIC method.

1. INTRODUCTION

The capability of electromagnetic wave to penetrate through the building walls has made through-the-wall imaging (TWI) of increasing importance in many civilian and military applications. The detection and localization of targets behind the wall is particularly useful in such applications as tracking of hostages and suspects inside

buildings, surveillance and reconnaissance, law enforcement, and various earthquake and avalanche rescue missions, to name a few [1–6].

For TWI, one needs not only to know if there is any target behind the wall but also where the target is located. Previously, several effective TWI algorithms have been proposed to address this problem. A non-coherent approach based on the trilateration technique is proposed for the localization of targets behind the wall in [7]. The delay-and-sum beamforming algorithm is proposed in [4] for the coherent processing of the measured data for TWI. The delay-and-sum beamforming algorithm incorporates the time delay, associated with the wave traveling through the wall, into the beamformer and is preferable for many real time imaging applications due to its fast computation speed. In order to build an accurate EM model, the Contrast Source Inversion (CSI) method is employed for TWI in [6] which is based on optimization and needs to be solved iteratively thus making it very time consuming. Linear inverse scattering algorithms based on the first order Born approximation that exploit the layered medium Green's function for TWI are studied in [1, 3, 5], resulting in a good compromise between the imaging accuracy and efficiency. In this paper, we focus on TWI within the framework of time reversal (TR) imaging. In particular, the Time Reversal Multiple Signal Classification (TR-MUSIC) method is employed for target detection and localization behind the wall.

Time reversal (TR) was first proposed in acoustics in [8, 9]. It has a range of applications, including acoustic imaging, nondestructive evaluation, destruction of tumors and kidney stones and underwater communication, etc [8–10]. Over the past decade, there has been increasing interest in applying time reversal techniques to electromagnetic waves for radar imaging, wireless communication, medical imaging and subsurface target detection [11–16]. The concept of TR is based on the invariance of the wave equation in lossless and stationary medium, i.e., if $E(r, t)$ is the solution to the wave equation in (1), $E(r, -t)$ is also the solution.

$$\nabla^2 E(r, t) - \mu\varepsilon \frac{\partial^2}{\partial t^2} E(r, t) = 0 \tag{1}$$

According to the wave equation, the reverse of the field in time domain (or phase conjugation in frequency domain) would precisely retrace the path of the original wave back to the source where it is excited. $E(r, t)$ is the divergent wave which we usually call scattered field while $E(r, -t)$ is the convergent wave which will focus on the source with physical or computational TR process. The physical TR of electromagnetic wave has been successfully validated experimentally in [15]. Due to the cost and complexity of physical TR,

computational TR is usually employed for radar imaging applications. TR imaging (TRI), decomposition of reverse time operator (D.O.R.T) and time reversal multiple signal classification (TR-MUSIC) are the three main computational TR imaging methods applied in radar imaging. TRI is the most direct and intuitional method for target localization. The procedure of standard TRI can be briefly summarized as follows [8, 9, 19]: first, radar transmits time domain signal to illuminate the unknown target; secondly, the scattered field from the target is measured by *an array* of receivers; thirdly, the received data is time reversed (or phase conjugated in frequency domain) and sent back to the same probing media from each receiver location; finally, the time reversed wave from different receivers converges towards the target and focuses at the target's position. The TRI for electromagnetic wave was first applied for freespace imaging and later for seismic imaging and landmine detection. In [17, 18] TRI is applied for TWI and good imaging results can be achieved by implementing TRI in Finite-Difference Time-Domain (FDTD) for different walls. Due to the backpropagation of the reversed field in TRI, the imaging resolution is still constrained to the diffraction limit. Meanwhile, the FDTD solver is employed for the time domain implementation of time reversal, the imaging process is very time consuming and the optimal focusing time should be determined by some strategy [20]. In the case of multiple scatterers TRI focuses more strongly on the dominant scatterer and masks the weaker scatters. As the standard TRI is iterated, final focused imaging result of only the strongest scatterer can only be achieved. Standard TR iteration does not allow focusing on weaker scatterers unless time-gating is applied. The D.O.R.T method overcomes this problem by exploiting the signal space of the multistatic response matrix and selectively focuses on different targets via different eigenvectors [12, 13, 21]. The D.O.R.T has been successfully applied for freespace and subsurface imaging, as well as medical imaging. Selective focusing on different target by D.O.R.T can be achieved for multiple scatterers. However, imaging quality degrades in the case of poorly-resolved targets. For an efficient dealing with this problem and also improving the imaging efficiency, the TR-MUSIC algorithm which exploits the null space of the multistatic response matrix was first proposed by Devaney in [22]. TR-MUSIC does not involve the FDTD solver for the implementation of the backpropagation of the time reversed field and thus is computationally very efficient. Simultaneously high resolution imaging of multiple scatterers with a high resolution can also be achieved with TR-MUSIC. TR-MUSIC was firstly proposed in acoustics and later applied in electromagnetic [22–26]. Most of the related works were originally focused on freespace

imaging and later on subsurface imaging. However, many practical applications, both military and commercial, are in the scenarios with target hidden behind an inaccessible obstacle, such as in through wall target detection and localization scenarios. Therefore, it is beneficial to carry out the analysis and extend the TR-MUSIC method in this case. In this paper, the TR-MUSIC method is applied for an efficient localization of multiple targets behind the wall by employing the layered medium Green's function for a homogeneous wall.

The organization of the remainder of this paper is as follows: in Section 2 TWI with TR-MUSIC is proposed and discussed. Formulas for TWI with TR-MUSIC are given in Section 2.1. An efficient evaluation of layered medium Green's function with the saddle point method is presented in Section 2.2. Several examples of targets localization behind the wall are presented in Section 3. And finally some conclusions and remarks are drawn in Section 4.

2. TWI WITH TR-MUSIC METHOD

Figure 1 shows a typical two dimensional scenario for multistatic radar TWI. We consider a uniform linear array of N elements centered at the position R_j at a distance of Z_S in front of the wall, where, $j = 1, 2, \ldots, N$, $R_j = (X_j, Z_j)$. The transceiver antenna elements are placed with an inter-element spacing Δx. Region I and III are freespace and Region II is the wall with complex dielectric constant ε_r and thickness d. A set of M point targets are located at position r_m in an inaccessible region behind the wall, where $m = 1, 2, \ldots, M$, $r_m = (x_m, z_m)$, $M < N$.
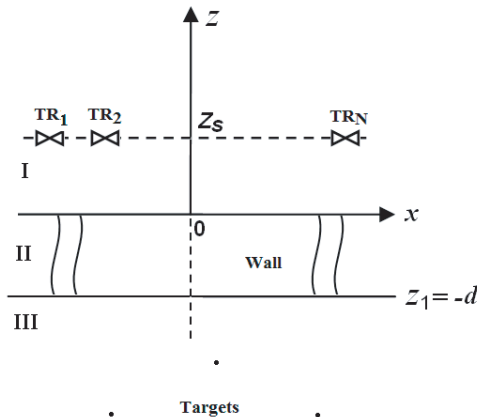

Figure 1. Measurement configuration of the multi-static radar TWI.

2.1. TR-MUSIC TWI

Assume each transceiver illuminate the targets with unit amplitude excitation. By employing the point target model and ignoring the multiple scattering effect between the targets, the received signal at the l-th antenna element is given by

$$v_l(\omega) = \sum_{j=1}^{N} \sum_{m=1}^{M} G(R_l, r_m, \omega) \tau_m G(r_m, R_j, \omega) \tag{2}$$

where τ_m is the scattering strength of the m-th target, G is the layered medium Green's function for the homogeneous wall.

To image the target TR-MUSIC exploits the multistatic response matrix K, whose element K_{ij} is defined as the scattered field detected at the i-th receiver due to the excitation of the j-th transmitter, can be derived as [22, 23]

$$K = \sum_{m=1}^{M} \tau_m g_m g_m^T \tag{3}$$

where $g_m(\omega) = [G(R_1, r_m, \omega) \; G(R_2, r_m, \omega), \cdots, G(R_N, r_m, \omega)]^T$.

According to the reciprocity principle $K_{ij} = K_{ji}$, the $N \times N$ multistatic response matrix is a symmetrical matrix. Both the D.O.R.T and TR-MUSIC are based on the singular value decomposition (SVD) of the K matrix:

$$K = U \Sigma V^H = \sum_{j=1}^{N} \sigma_j u_j v_j^H \tag{4}$$

where σ_j, u_j and v_j are the j-th singular value and the j-th column vector of the orthonormal matrices U and V, respectively. By performing SVD of the response matrix, the space C of the measurement data can be decomposed into the direct sum of signal subspace S and null subspace B: $C = S \oplus B$. S is spanned by the principal eigenvectors corresponds to the nonzero eigenvalues and B is spanned by the eigenvectors having zero eigenvalues, i.e.,

$$S = Span\{u_j, \sigma_j > 0\} \perp B = Span\{u_j, \sigma_j = 0\} \tag{5}$$

It has been demonstrated that the background Green's function vectors $\{g_m(\omega), m = 1, 2 \ldots, M\}$ forms a basis for the signal space S [22, 23]. Then from Eq. (5) one can get:

$$u_j^H g_m = 0, \quad \sigma_j = 0 \tag{6}$$

Suppose there are L none-zero eigenvalues of the response matrix, the locations of the scatterers can then be determined from the time-reversal MUSIC pseudo-spectrum,

$$p^{MUSIC}(r_p) = \frac{1}{\sum\limits_{i=L+1}^{N} |\langle u_i^*, g_p \rangle|^2} \tag{7}$$

The inner product $\langle u_i^*, g_p \rangle = 0$ when r_p matches with the true location of the target and it shows a peak at the target location.

Both D.O.R.T and TR-MUSIC are based on the SVD of the response matrix. However, D.O.R.T exploits the signal space and TR-MUSIC exploits the null space. In the case of poorly-resolved targets, the signal space eigenvectors becomes linear combination of the background Green's function vectors. Backpropagation of such non-independent eigenvectors creates overlapped wavefronts and causes image degradation in D.O.R.T. However, in TR-MUSIC, regardless of the well-resolvedness criteria, the null space is always orthogonal to the signal space resulting in a much higher resolution imaging result than D.O.R.T method even for poorly-resolved targets.

2.2. Evaluation of the Layered Medium Green's Function

For the calculation of the time-reversal MUSIC pseudo-spectrum in Eq. (7) an efficient evaluation of the layered medium Green's function for the TWI is required. For the three layered medium shown in Fig. 1, we denote the wave numbers in Region I and III as k_1 and in region II as k_2, $k_1 = 2\pi f/c$, $k_2 = k_1\sqrt{\varepsilon_r}$, c is the speed of light and f is the working frequency. For the homogeneous wall shown in Fig. 1, the spectrum form of the layered medium Green's function can be written as [25]:

$$G(R_l, r_m, \omega) = \frac{j}{4\pi} \int_{-\infty}^{\infty} dk_x T(k_x) \frac{\exp(jk_x(X_l - x_m) + jk_{1z}(Z_l - z_m - d))}{k_{1z}} \tag{8}$$

where T is the transmission coefficient for the three-layered medium, in particular [27],

$$T(k_x) = \frac{(1 - R_{12}^2)\exp(jk_{2z}d)}{1 - R_{12}^2\exp(j2k_{2z}d)}, \quad R_{12} = \frac{k_{1z} - k_{2z}}{k_{1z} + k_{2z}} \tag{9}$$

$$k_{1z} = \sqrt{k_1^2 - k_x^2}, \quad k_{2z} = \sqrt{k_2^2 - k_x^2}$$

By substituting Eq. (9) into Eq. (8), the layered medium Green's

function can be expressed as:

$$G(R_l, r_m, \omega) = \frac{j}{4\pi} \int_{-\infty}^{\infty} dk_x \frac{\left(1 - R_{12}^2\right)}{\left(1 - R_{12}^2 \exp(-j2k_{2z}z_1)\right) k_{1z}}$$
$$\cdot \exp(-jk_{2z}z_1 + jk_x(X_l - x_m) + jk_{1z}(Z_l - z_m + z_1)) \quad (10)$$

As is shown in Fig. 1, z_1 is the position of the back of the wall in the z direction. For TWI an efficient evaluation of the above integral is required for the real time processing of the data. During the long computation time of the Sommerfeld-type integral in (10), the moving of the target may cause smearing of the image and displacement of the target. In this paper, the saddle point method is employed for the asymptotic evaluation of the integral in Eq. (10). For the simplification of Eq. (10) we denote

$$F(k_x) = \frac{\left(1 - R_{12}^2\right)}{\left(1 - R_{12}^2 \exp(-j2k_{2z}z_1)\right) k_{1z}} \quad (11)$$

$$\Phi(k_x) = -k_{2z}z_1 + k_x(X_l - x_m) + k_{1z}(Z_l - z_m + z_1) \quad (12)$$

Then Eq. (10) can be simplified as

$$G(R_l, r_m, \omega) = \frac{j}{4\pi} \int_{-\infty}^{\infty} dk_x F(k_x) \exp(j\Phi(k_x)) \quad (13)$$

The stationary phase point can be determined from $\Phi'(k_x) = 0$, which gives the following equation:

$$\frac{k_x}{k_{2z}}z_1 - \frac{k_x}{k_{1z}}(Z_l - z_m + z_1) + |X_l - x_m| = 0 \quad (14)$$

The solution of the above equation is the stationary phase point k_{x0}. Using the Taylor series expansion the phase item can be written as

$$\Phi(k_x) \cong \Phi(k_{x0}) + \frac{1}{2}\Phi''(k_{x0})(k_x - k_{x0})^2 \quad (15)$$

where $\Phi'' = \frac{k_2^2 z_1}{k_{2z}^3} - \frac{k_2^2(Z_l - z_m + z_1)}{k_{1z}^3}$.

Assuming that $\varphi(x)$ is a high oscillating function, the following form integral can be efficiently approximated with saddle point method as [27]:

$$I = \int_{-\infty}^{\infty} F(x)e^{-j\varphi(x)}dx = \sqrt{\frac{2\pi}{j|\Phi''(x_0)|}}F(x_0)e^{-j\varphi(x_0)} \quad (16)$$

where the x_0 is the stationary phase point. By employing the saddle point method, the layered medium Green's function in Eq. (13) can be

derived as

$$
\begin{aligned}
G(R_l, r_m, \omega) &= \frac{j}{4\pi} F(k_{x0}) \exp(j\Phi(k_{x0})) \int_{-\infty}^{\infty} dk_x \\
&\quad \exp\left(j\frac{1}{2}\Phi''(k_{x0})(k_x - k_{x0})^2\right) \\
&= \frac{j}{4} F(k_{x0}) \exp(j\Phi(k_{x0})) \sqrt{\frac{2}{\pi |\Phi''(k_{x0})|}} e^{j\pi/4} \quad (17)
\end{aligned}
$$

Finally, the Green's function vector the calculation of time-reversal MUSIC pseudo-spectrum in Eq. (7) can be derived as

$$
g_p = [G(R_1, r_p, \omega) \;\; G(R_2, r_p, \omega), \ldots, G(R_N, r_p, \omega)]^T \quad (18)
$$

3. SIMULATION RESULTS

In order to show the effectiveness of TR-MUSIC method as applied to TWI problems, some numerical simulation results are presented in this section. The calculation of the background Green's function vectors is essential for the TR-MUSIC application to TWI. In order to show the effectiveness of efficient evaluation of the layered medium Green's function, we first present some results for the calculation of Green's function. By setting Region II in Fig. 1 to be freespace, the layered medium Green's function reduces to the freespace case, i.e., $\varepsilon_r = 1$. Fig. 2 plots the Green's function vector in Eq. (18) using the numerical evaluation of Sommerfield integral in (13) and the saddle point method solution in Eq. (17). For the convenience of comparison the theoretical freespace Green's function (in the form of Hankel function) is also
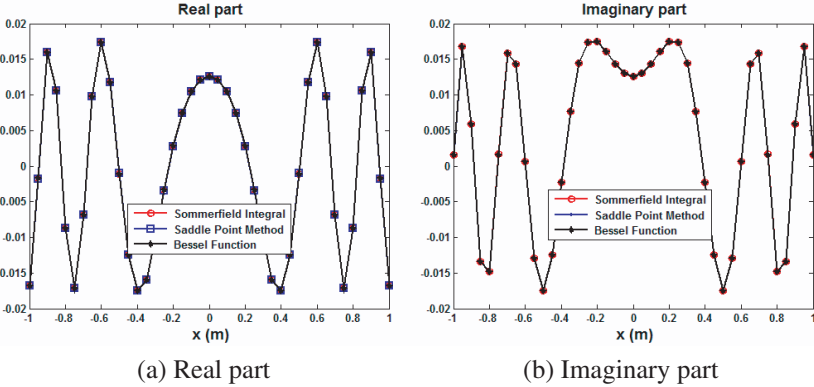

(a) Real part   (b) Imaginary part

Figure 2. Freespace Green's function calculation result.

preseented in Fig. 2. The operating frequency is $3\,\mathrm{GHz}$, $r_p = (0, -1\,\mathrm{m})$, $Z_i = 0.5\,\mathrm{m}$ and X_i is uniformly distributed from $-1\,\mathrm{m}$ to $1\,\mathrm{m}$ with a step $0.05\,\mathrm{m}$, $i = 1, 2, \ldots, N$. From the real and imaginary part of the Green's function shown in Fig. 2 we could see that the result evaluated with the saddle point method agrees very well with the theoretical and Sommerfield integral results.

Figure 3 is the Green's function for a homogeneous wall whose parameters are $\varepsilon_r = 6$, $\sigma = 0.01\,\mathrm{S/m}$ and $d = 0.2\,\mathrm{m}$. The other parameters are the same as previous simulation. From the real and imaginary parts of the layered medium Green's function in Fig. 3 we could see that the result evaluated using Eq. (17) agrees very well with the numerical Sommerfield integral result. However, the computation time for the Sommerfield integral is $3.041\,\mathrm{s}$ while the saddle point method takes only $0.016\,\mathrm{s}$. The efficient evaluation of the layered

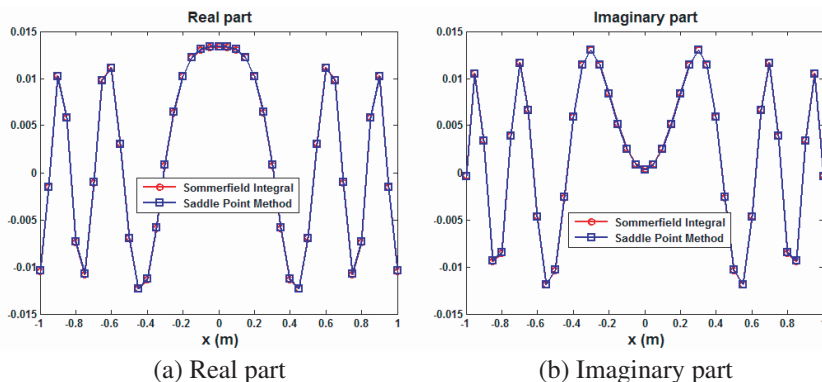(a) Real part   (b) Imaginary part

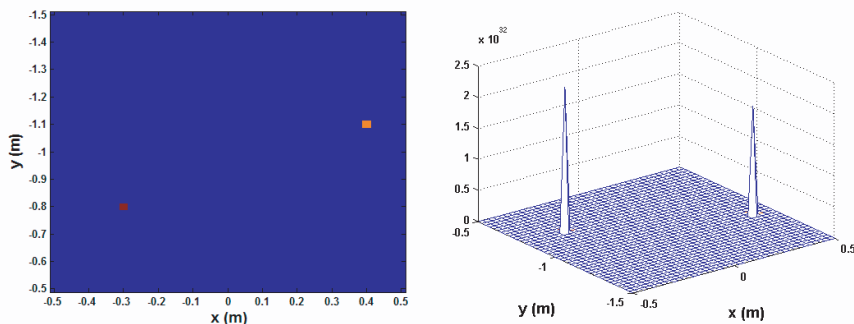**Figure 3.** Layered medium Green's function calculation result.

Figure 4. TR-MUSIC through-wall localization of two well-resolved targets: (a) TR-MUSIC pseudo-spectrum; (b) mesh plot of the TR-MUSIC pseudo-spectrum.

medium Green's function is indeed very useful for real time TWI.

    With the efficient evaluation of the background medium Green's function, the time-reversal MUSIC pseudo-spectrum can be calculated for each image pixel and the peaks of the pseudo-spectrum indicate the locations of the targets. In order to show the effectiveness of TWI with TR-MUSIC, the imaging result of two well-resolved targets is presented in Fig. 4. The two targets are located at $(-0.3\,\mathrm{m},\ -0.8\,\mathrm{m})$ and $(0.4\,\mathrm{m},\ -1.1\,\mathrm{m})$. The operating frequency is $3\,\mathrm{GHz}$; the transceivers are uniformly distributed from $-1\,\mathrm{m}$ to $1\,\mathrm{m}$ with a step $0.05\,\mathrm{m}$ at a distance of $0.3\,\mathrm{m}$ from the front wall. The dielectric constant, conductivity and thickness of the wall are $\varepsilon_r = 6$, $\sigma = 0.01\,\mathrm{S/m}$ and $d = 0.2\,\mathrm{m}$. From the
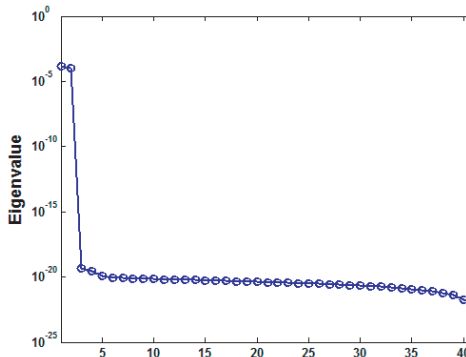

Figure 5. Eigenvalues of the multistatic response matrix of two well resolved point targets.
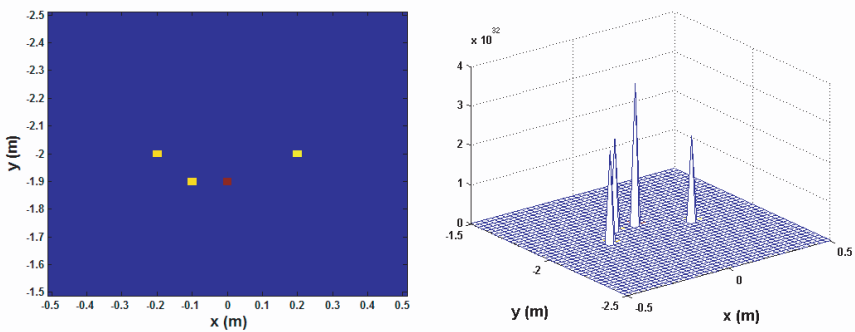

Figure 6. TR-MUSIC through-wall localization of four closely space targets: (a) TR-MUSIC pseudo-spectrum; (b) mesh plot of the TR-MUSIC pseudo-spectrum.

pseudo-spectrum plotted in Fig. 4 we could see that TR-MUSIC gives a very good simultaneous localization of the two targets with much higher resolution than either TRI or D.O.R.T method. Fig. 5 is the eigenvalues of the multistatic response matrix in Eq. (3). From this figure we could find that for the two point targets there are only two non-zeros eigenvalues for the response matrix, each one is associated with one target. In order to show the performance of TR-MUSCI for the localization of poorly-resolved targets, the imaging result of four closely space point targets is presented in Fig. 6. The operational conditions are the same as previous simulation except that the four point targets are located at $(-0.2\,\text{m}, -2\,\text{m})$, $(-0.1\,\text{m}, -1.9\,\text{m})$, $(0, -1.9\,\text{m})$ and $(0.2, -2\,\text{m})$, respectively. For the closely spaced targets we could see that TR-MUSIC still gives very good localization for all the targets. Fig. 7 plots the eigenvalues of the multistatic response matrix for the four point targets. From this figure we could see that for the four point targets in this simulation there are four significant non-zeros eigenvalues for the response matrix. Through backpropagation of the eigenvectors associated with each non-zeros eigenvalues the D.O.R.T selectively focuses on each target. However, TR-MUSIC exploits the null space and achieves simultaneous localization of all the targets with much higher resolution.

The above simulations are carried out for the point target localization. In the final example the imaging result of two PEC square objects are presented. The two PEC square targets whose size are $0.2\,\text{m}$ by $0.2\,\text{m}$ are centered at $(-0.3\,\text{m}, -2\,\text{m})$ and $(0.1\,\text{m}, -2\,\text{m})$. The other conditions remain the same as previous simulation. The localization of spatial extended targets can be achieved by properly setting a break point in the singular curves of the multistatic response matrix. For
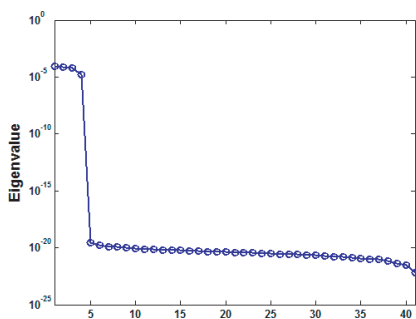

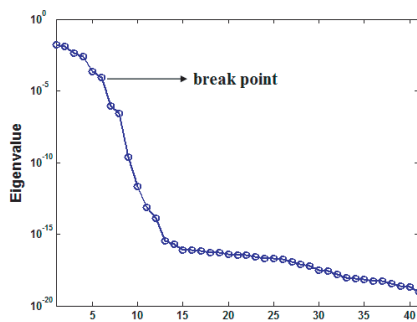**Figure 7.** Eigenvalues of the multistatic response matrix of four closely spaced point targets.

Figure 8. Eigenvalues of the multistatic response matrix of two PEC squares.
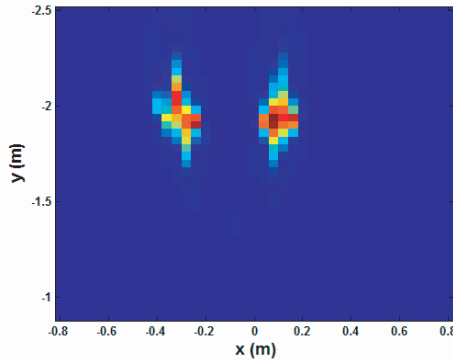
Figure 9. TR-MUSIC through-wall localization of two PEC squares.

the two PEC squares in this simulation, the singular values are plotted
in Fig. 8. For the calculation of the TR-MUSIC pseudo-spectrum in
Eq. (7) the break point is chosen as $L = 6$ where the seventh eigenvalues
significantly drops to zero. By using the eigenvectors correspond to
the eigenvalues after the break point, the imaging result of the two
PEC squares is shown in Fig. 9. From this figure we could see that
for spatially extended targets TR-MUSIC could still well localized the
two targets.

4. CONCLUSION

Previously, the TRI and D.O.R.T method have been successfully
applied for freespace and subsurface imaging. Many practical
applications, however, consists of scenarios with target hidden behind
obstacles or visually opaque materials, such as through wall target
detection and localization. In this paper, the TR-MUSIC method
is extended for these applications. TR-MUSIC does not involve the
FDTD solver for the implementation of the backpropagation of the
time reversed field and is very computational efficient. The Green's
function vectors for the computation of the TR-MUSIC pseudo-
spectrum is efficiently evaluated with the saddle point method for a
homogeneous wall. By employing the null space of the multistatic
response matrix, simultaneous localization of multiple targets behind
the wall can be achieved by TR-MUSIC method. Presented numerical
results clearly demonstrate the effectiveness of the TR-MUSIC method
in TWI applications.

ACKNOWLEDGMENT

REFERENCES

1. Dehmollaian, M. and K. Sarabandi, "Refocusing through building walls using synthetic aperture radar," *IEEE Trans. Geosci. Remote Sensing*, Vol. 46, No. 6, 1589–1599, 2008.

2. Wang, G. and M. Amin, "Imaging through unknown walls using different standoff distances," *IEEE Trans. Signal Processing*, Vol. 54, No. 10, 4015–4025, 2006.

3. Soldovieri, F. and R. Solimene, "Through-wall imaging via a linear inverse scattering algorithm," *IEEE Geosci. Remote Sensing Lett.*, Vol. 4, No. 4, 513–517, 2007.

4. Ahmad, F., M. G. Amin, and S. A. Kassam, "Synthetic aperture beamformer for imaging through a dielectric wall," *IEEE Trans. Aerospace and Electronic Systems*, Vol. 41, 271–283, 2005.

5. Soldovieri, F., G. Prisco, and R. Solimene, "A multi-array tomographic approach for trough-wall Imaging," *IEEE Trans. Geosci. Remote Sensing*, Vol. 46, No. 4, 1192–1199, 2008.

6. Song, L. P., C. Yu, and Q. H. Liu, "Through-wall imaging (TWI) by radar: 2-D tomographic results and analyses," *IEEE Trans. Geosci. Remote Sensing*, Vol. 43, No. 12, 2793–2798, 2005.

7. Ahmad, F. and M. G. Amin, "Noncoherent approach to through-the-wall radar localization," *IEEE Trans. Aerospace and Electronic Systems*, Vol. 42, No. 4, 1405–1419, 2006.

8. Fink, M., D. Cassereau, A. Derode, C. Prada, P. Roux, M. Tanter, J. Thomas, and F. Wu, "Time-reversed acoustics," *Rep. Prog. Phys*, Vol. 63, 1933–1995, 2000.

9. Fink, M. and C. Prada, "Acoustic time-reversal mirrors," *Inverse Problems*, Vol. 17, R1–R38, 2001.

10. Hristova, Y., P. Kuchment, and L. Nguyen, "Reconstruction and time reversal in thermoacoustic tomography in acoustically homogeneous and inhomogeneous media," *Inverse Problems*, Vol. 24, 1–25, 2008.

11. Devaney, A. J., "Time reversal imaging of obscured targets from multistatic data," *IEEE Trans. Antennas Propag.*, Vol. 53, No. 5, 1600–1610, 2005.

12. Micolau, G., M. Saillard, and P. Borderies, "DORT method as

applied to ultrawideband signals for detection of buried objects," *IEEE Trans. Geosci. Remote Sensing*, Vol. 41, No. 8, 1813–1820, 2003.

13. Yavuz, M. and F. L. Texeira, "Full time-domain DORT for ultrawideband electromagnetic fields in dispersive, random inhomogeneous media," *IEEE Trans. Antennas Propag.*, Vol. 54, No. 8, 2305–2315, 2006.

14. Liu, D., G. Kang, L. Li, Y. Chen, S. Vasudevan, W. Joines, Q. H. Liu, J. Krolik, and L. Carin, "Electromagnetic time-reversal imaging of a target in a cluttered environment," *IEEE Trans. Antennas and Propagation*, Vol. 53, No. 9, 3058–3066, 2005.

15. Lerosey, G., J. Rosny, A. Tourin, A. Derode, G. Montaldo, and M. Fink, "Time Reversal of Electromagnetic Waves," *Physical Review Letters*, Vol. 92, No. 19, 1–3, 2003.

16. Liu, X.-F., B.-Z. Wang, S.-Q. Xiao, and J. H. Deng, "Performance of impulse radio UWB communications based on time reversal technique," *Progress In Electromagnetics Research*, Vol. 79, 401–413, 2008.

17. Zheng, W., Z. Zhao, and Z.-P. Nie, "Application of TRM in the UWB through wall radar," *Progress In Electromagnetics Research*, Vol. 87, 279–296, 2008.

18. Zheng, W., Z. Zhao, Z.-P. Nie, and Q. H. Liu, "Evaluation of TRM in the complex through wall environment," *Progress In Electromagnetics Research*, Vol. 90, 235–254, 2009.

19. Borcea, L., G. Papanicolaou, C. Tsogka, and J. Berryman, "Imaging and time-reversal in random media," *Inverse Problems*, Vol. 18, 1247–1279, 2002.

20. Kosmas, P. and C. Rappaport, "Time reversal with the FDTD method for microwave breast cancer detection," *IEEE Trans. Microw. Theory Tech.*, Vol. 53, No. 7, 2317–2323, 2005.

21. Prada, C., S. Manneville, D. Spoliansky, and M. Fink, "Decomposition of the time reversal operator: Detection and selective focusing on two scatterers," *J. Acoust. Soc. Am.*, Vol. 99, No. 4, 2067–2076, 1996.

22. Lev-Ari, H. and A. J. Devaney, "The time-reversal technique reinterpreted: Subspace-based signal processing for multi-static target location," *IEEE Sensor Array and Multichannel Signal Processing Workshop*, 509–513, Cambridge, USA, 2000.

23. Devaney, A. J., E. A. Marengo, and F. K. Gruber, "Time-reversal-based imaging and inverse scattering of multiply scattering point targets," *J. Acoust. Soc. Am.*, Vol. 118, No. 5, 3129–3138, 2005.

24. Davy, M., J.-G. Minonzio, J. de Rosny, C. Prada, and M. Fink, "Influence of noise on subwavelength imaging of two close scatterers using time reversal method: Theory and experiments," *Progress In Electromagnetics Research*, Vol. 98, 333–358, 2009.

25. Marengo, E. A., F. K. Gruber, and F. Simonetti, "Time-reversal MUSIC imaging of extended targets," *IEEE Trans. Image Processing*, Vol. 16, 1967–1984, 2007.

26. Baussard, A. and T. Boutin, "Time-reversal RAP-MUSIC imaging," *Waves in Random and Complex*, Vol. 18, 151–160, 2008.

27. Chew, W. C., *Waves and Fields in Inhomogeneous Media*, Chapter 2, IEEE Press, Piscataway, NJ, 1997.